energies

MDPI

Article

Comparative Study of the NO_x, CO Emissions, and Stabilization Characteristics of H_2-Enriched Liquefied Petroleum Gas in a Swirl Burner

Abay Mukhamediyarovich Dostiyarov [1], Dias Raybekovich Umyshev [1,2,*], Zhanar Abdeshevna Aidymbayeva [1], Ayaulym Konusbekovna Yamanbekova [1], Zhansaya Serikkyzy Duisenbek [1], Madina Bakytzhanovna Kumargazina [1], Nurlan Rezhepbayevich Kartjanov [3] and Ainur Serikbayevna Begimbetova [4]

[1] Department of Thermal Engineering, Institute of Energy and Green Technologies, Energo University After Gumarbek Daukeev, Almaty 050013, Kazakhstan; z.aidymbayeva@aues.kz (Z.A.A.); a.yamanbekova@aues.kz (A.K.Y.); z.duisenbek@aues.kz (Z.S.D.)
[2] Department of Power Engineering, Institute of Energy and Mechanical Engineering, Satpayev University, Almaty 050013, Kazakhstan
[3] Department of Thermal Power Engineering, L.N. Gumilyov Eurasian National University, Astana 010000, Kazakhstan; nurlanke16@gmail.com
[4] Department of Life Safety and Environmental Protection, Institute of Energy and Green Technologies, Energo University After Gumarbek Daukeev, Almaty 050013, Kazakhstan; a.begimbetova@aues.kz
* Correspondence: d.umyshev@satbayev.university

Abstract: The global shift toward renewable fuels and the reduction in anthropogenic environmental impact have become increasingly critical. However, the current challenges in fully transitioning to environmentally friendly fuels necessitate the use of transitional fuel mixtures. While many alternatives have been explored, the combination of hydrogen and LPG appears to be the most practical under the conditions specific to Kazakhstan. This study presents experimental findings on a novel burner system that utilizes the airflow swirl and hydrogen enrichment of LPG. It evaluates the effects of hydrogen addition, fuel supply methods, and swirl intensity—achieved by adjusting the outlet vanes—on flame stabilization as well as NO_x and CO emissions. The results show that the minimum NO_x concentration achieved was 12.08 ppm, while the minimum CO concentration was 101 ppm. Flame stabilization studies indicate that supplying the fuel at the center of the burner, rather than at the base, improves stabilization by 23%. Additionally, increasing the proportion of hydrogen positively affects stabilization. However, the analysis also reveals that, as the hydrogen content in the fuel rises, NO_x concentrations increase. These findings highlight the importance of balancing the hydrogen enrichment, airflow swirl, and fuel supply methods to achieve optimal combustion performance. While hydrogen-enriched LPG offers enhanced flame stabilization, the associated rise in NO_x emissions presents a challenge that requires careful management to maintain both efficiency and environmental compliance.

Keywords: LPG; swirl; hydrogen; combustion; enrichment

Citation: Dostiyarov, A.M.; Umyshev, D.R.; Aidymbayeva, Z.A.; Yamanbekova, A.K.; Duisenbek, Z.S.; Kumargazina, M.B.; Kartjanov, N.R.; Begimbetova, A.S. Comparative Study of the NO_x, CO Emissions, and Stabilization Characteristics of H_2-Enriched Liquefied Petroleum Gas in a Swirl Burner. *Energies* **2024**, *17*, 6132. https://doi.org/10.3390/en17236132

Academic Editors: Cunxi Liu and Qiang An

Received: 26 September 2024
Revised: 22 October 2024
Accepted: 25 October 2024
Published: 5 December 2024

1. Introduction

Review and Analysis

Currently, the issue of reducing CO_2 emissions is becoming increasingly relevant. In particular, Kazakhstan has adopted a law on carbon neutrality [1]. According to the law, gas will be used as a transitional energy source, with plans to eventually switch to alternative energy sources. The document pays special attention to hydrogen; specifically, the final demand will shift toward the use of low-carbon fuels (biofuels and hydrogen) in areas where the transition to electricity remains difficult. In this regard, a long-term vision for the development of hydrogen energy will be formulated. Therefore, the use of hydrogen

mixed with different gases is an urgent task. The authors emphasized pre-mixing, as this is considered the most environmentally friendly type of fuel combustion [2]. Research on the combustion of pre-mixed hydrogen is critical [3,4], particularly because hydrogen is a highly explosive fuel [3].

Studies on the combustion of pre-prepared hydrogen–air mixtures [3] at various cross-sections show an increase in the combustion rate as the longitudinal cross-section of the combustion zone decreases. Studies of a partially mixed hydrogen and natural gas mixture [4] revealed that increasing the proportion of hydrogen reduces the flame size. Research on a dimethyl ether and hydrogen mixture showed that the maximum concentration of NO_x occurs at a hydrogen volume concentration of 15% [5]. Another study on the addition of water droplets to a mixed hydrogen–air mixture demonstrated that changing the equivalence ratio has an insignificant effect on the laminar combustion rate [6]. An investigation of flame stabilization and structure in a new type of burner [7] identified a region where diffusion and mixed flames converge, known as the cold rim thermal zone. This finding is important since mixing within the burner can be uneven. Studies of non-premixed hydrogen jet flames [8] revealed a certain limit to the hydrogen concentration beyond which the flame does not grow. Research on the addition of hydrogen to pre-mixed fuel [9] indicates that hydrogen addition does not affect lean blowout (LBO) at a value of $\varphi \sim 0.5$. The authors also noted that increasing the hydrogen proportion leads to a rise in CO and UHC concentrations due to the delayed reactivity of hydrogen. The secondary addition of hydrogen to a swirling flame [10] showed that increasing the hydrogen content results in higher NO_x concentrations but lower CO levels in the exhaust gases. The addition of hydrogen significantly improved flame stabilization. A study of gas recirculation and methane addition in lean premixed hydrogen flames [11] also showed improved flame stabilization. Research on ammonia and hydrogen combustion in premixed flames [12] found that adding ammonia to hydrogen at a constant φ value slightly reduces the adiabatic temperature of the gases but increases the thermal thickness of the flame. This is significant because an increase in flame size affects the CO and UHC concentrations. Studies of NO_x emissions in premixed hydrogen flames [13] showed that the concentration of NO_2 during hydrogen combustion is three times lower than that of NO in all combustion modes. Research on combustion and NO_x formation in a burner with a partially premixed hydrogen mixture [14] demonstrated that increasing mixing at $\varphi < 0.85$ reduces NO_x concentrations. Additionally, it was shown that higher relative humidity leads to a further reduction in NO_x formation.

A study on the combustion of a biodiesel and hydrogen mixture [15] found that adding hydrogen at a volume of 7.5 LPM to a mixture of transformer oil and biodiesel increased the brake thermal efficiency by 37.3%, reduced fuel consumption by 15.33%, decreased CO emissions by 27.09%, and lowered unburned hydrocarbons (UHCs) by 28.53%.Investigations into ignition processes [16] during hydrogen combustion demonstrated that pre-mixing results in a higher reaction rate, with a 1–2 s delay between ignition in comparison to non-premixed cases. The addition of a hydrogen–LPG mixture to an internal combustion engine [17] resulted in a reduction in CO and NO_x concentrations as the hydrogen proportion increased. Specifically, increasing the hydrogen proportion reduced NO_x concentrations by 1.89%. Several noteworthy studies on hydrogen engines have been conducted by the authors of [18–20], demonstrating that hydrogen use increases engine power while ensuring compliance with Euro V standards.

A study on the addition of hydrogen to a methane–air mixture in a new swirl burner [21] showed that, for an equivalence ratio of 0.5 to 0.73, adding 20% hydrogen did not alter the NO_x concentrations. However, increasing the equivalence ratio led to higher NO_x concentrations, suggesting that the increase in oxygen proportion, combined with the higher combustion temperature from hydrogen, promotes NO_x formation. Studies on the combustion of an LPG mixture in a staged swirl combustor revealed that flame stabilization and NO_x concentrations are significantly influenced by the swirl degree [22]. Both stages played an essential role, with maximum NO_x concentrations observed at an

external swirl angle of 60° and an internal angle of 30°, while the lowest concentrations were achieved with a 60° angle across all φ options A detailed analysis of hydrogen combustion in swirling flames [23] indicated that, as the proportion of hydrogen increases, the flame shifts monotonously toward the outlet due to flame turbulence. Studies of premixed CH_4/H_2 flames [24] revealed that, at φ = 0.8 and with a hydrogen proportion of 20%, CO_2 concentrations decreased by 10%, although NO_x concentrations rose by 2%. Notably, in lean mixtures, the concentrations of harmful substances decrease, with maximum NO and NO_2 concentrations of 2107 ppm and 84 ppm, respectively.

The analysis shows that a significant amount of research has been conducted on premixed hydrogen combustion. However, relatively few studies have focused on the combustion of hydrogen and LPG in a swirl burner within the equivalence ratio range of 0.17–1.00. Most studies have been typically conducted on internal combustion engines, where combustion occurs at pressures above atmospheric levels. This article introduces the new following areas of research:

1. A new type of burner device is used, where the flow is swirled at both the inlet and outlet of the burner;
2. A wide range of hydrogen proportions in LPG is used—up to 40%;
3. The dependencies of NO_x and CO concentrations on the proportion of the hydrogen and the angle of the outlet blades during the pre-mixing of hydrogen and LPG are studied.

The importance of the study lies in determining the influence of the hydrogen fraction, flow swirl, and fuel intake method on such characteristics as NO_x and CO concentrations as well as flame stabilization.

2. Materials and Methods

Figure 1 illustrates the methodology of the experimental studies. As shown in the figure, the independent variables are the air flow, LPG, and hydrogen flow rates, as well as the blade angle. The dependent variables are the concentrations of NO and CO. The dimensions of the burner device are provided in Table 1, and the experimental conditions are presented in Table 2.

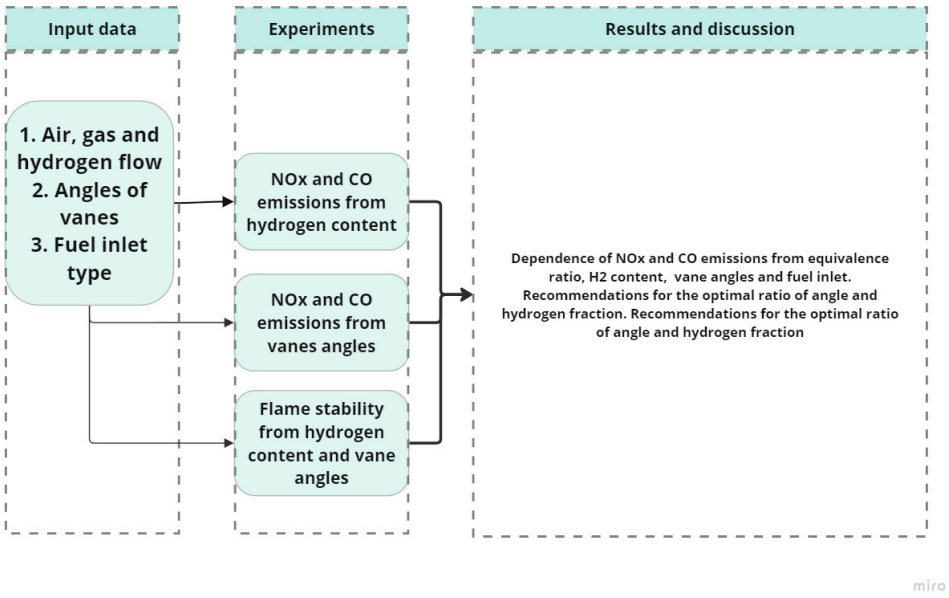

Figure 1. Experimental research methodology.

Table 1. The dimensions of the burner device [25].

Parameter	Units	Value
Length	mm	350
Inlet diameter	mm	50
Outlet diameter	mm	200

Table 2. Experimental conditions [25].

Parameter	Units	Value
Ambient temperature	°C	20
Air humidity	%	40
Equivalence ratio	-	0.17–1.00
Reynolds number	-	50,000–350,000
X_{H2} (volume%)	γ, %	0–40
Air flow	m^3/s	0.19–1.19
LPG flow	m^3/s	0.0105
Hydrogen flow	m^3/s	0–0.0036
LPG	-	C_3H_8—50%, C_4H_{10}—50%
Hydrogen	-	H_2; 99.96% purity
Air viscosity	m^2/s	15.06×10^{-6}
Swirl number (SW)	-	30°—0.4; 45°—0.8; 60°—1.3

The burner device consists of five main elements: inlet vanes with an angle of 45°, a fuel supply tube, outlet blades, and holes for fuel supply located at the base of the outlet vanes [25].

To calculate the equivalence ratio, the following formula was used [25]:

$$\varphi = \frac{\frac{m_{fuel}}{m_{air}}}{\left(\frac{m_{fuel}}{m_{air}}\right)_{stoich.}} \quad (1)$$

where φ—is equivalence ratio, $\frac{m_{fuel}}{m_{air}}$—fuel-to-air ratio, *stoich.*—stoichiometry.

Hydrogen fraction was calculated by Formula (2) [25]:

$$\gamma = \frac{H_2}{H_2 + LPG} \quad (2)$$

where γ—hydrogen fraction, H_2—hydrogen flow, LPG– LPG flow.

The swirl number was calculated by formula [25]:

$$SW = \frac{2}{3}\left[\frac{1 - \left(\frac{R_h}{R}\right)^3}{1 - \left(\frac{R_h}{R}\right)^2}\right] tan\beta \quad (3)$$

where R_h—hydrogen fraction, R_h—hyb radius, R—outer radius, β—angle of outlet vanes.

Reynolds number was calculated by formula [25]:

$$Re = \frac{\omega \cdot d}{\nu} \quad (4)$$

where ω—velocity, d—diameter, and ν—viscosity.

Table 3 presents the initial conditions and outlines the main parameters used in the experiments. In a previous experiment [25], LPG was supplied through a fuel supply tube, while hydrogen was fed through holes at the base of the outlet vanes. In this experiment, two methods for feeding the pre-mixed LPG+H_2 were considered: in the first method, the mixture was supplied through holes on the fuel tube, and in the second method, through

holes at the base of the outlet vanes. The diagram of the burner device is shown in Figure 2. The burner was developed based on patents obtained in the Republic of Kazakhstan [26,27]. The equipment error margin is presented in Table 4.

Table 3. Initial conditions.

Fuel Supply	Place
Type 1	Fuel tube
Type 2	Base of the outlet vanes

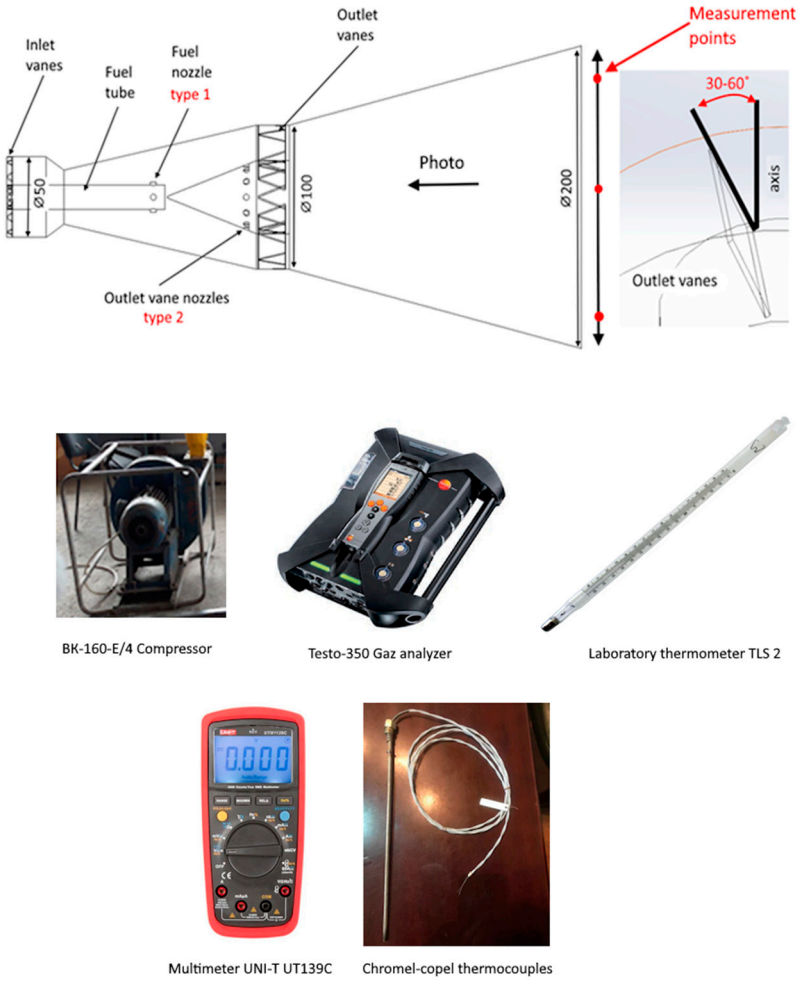

Figure 2. Experimental burner device and equipment.

Table 4. Equipment and error margin.

Equipment	Absolute Error	Relative Error σ, %
Laboratory thermometers	±1.0 °C	0.16
Chromel–copel thermocouples	In the range from minus 40 to plus 375 °C: ±1.5	0.4
Gas analyzer	NO_x: abs. ± 2 ppm with measured values from 0 to 39.9 ppm	5
	CO: ±10 ppm	1
	Temperature: ±1.0 °C	0.16

The measurement error of the instruments is defined as the sum of all the errors of the instruments:

$$\sigma_{m.} = \sqrt{{\sigma_{thermometer}}^2 + {\sigma_{thermocouple}}^2 + {\sigma_{NOx}}^2 + {\sigma_{CO}}^2} = 5.12\% \quad (5)$$

where ${\sigma_{thermometer}}^2$ denotes the relative error of thermometers, ${\sigma_{thermocouple}}^2$ denotes the relative error of the thermocouple, ${\sigma_{NOx}}^2$ denotes the relative error of the NO_x measurements, ${\sigma_{CO}}^2$ denotes the relative error of CO measurements.

The standard deviation of the measurements is calculated as follows:

$$s = \sqrt{\frac{\delta_1^2 + \delta_1^2 + \delta_1^2 + \delta_1^2}{N-1}}$$

where δ_1^2 denotes the deviation of the measurements.

The standard deviation of the mean measurements is as follows:

$$\sigma_x = \frac{s}{\sqrt{N}}$$

The standard deviation of the measurements are presented in Table 5.

Table 5. Uncertainty analysis on the results.

Measurement	Standard Deviation
NOx	±0.2 ppm
CO	±19.34 ppm

3. Results

3.1. Flame Stabilization

Figure 3 shows the dependence of the lean blowoff (LBO) on the equivalence ratio, vane angle, hydrogen fraction, and fuel feed type. For both configurations (Type 1 and Type 2), an increase in the hydrogen fraction and velocity results in improved flame stabilization. For Type 1, at a vane angle of 30°, high stabilization is achieved at lower speeds. However, increasing the hydrogen fraction leads to a rise in flame temperature, but as the velocity reaches 15 m/s, the stabilization indicators decline. At the same hydrogen concentration and at a vane angle of 30°, an increase in velocity results in an 8% decrease in stabilization. For every 10% increase in the hydrogen fraction, flame stabilization improves by an average of 32%. Increasing the vane angle to 45° further enhances the flame stabilization. At a hydrogen concentration of 30%, φ_{LBO} values for 30° and 45° are 0.23 and 0.25, respectively. This improvement is due to more efficient fuel–air mixing in the reverse flow zones formed behind the outlet vanes. These findings are consistent with previous studies [25] and those reported in [28]. The increase in stabilization is also associated with the high heat of combustion of the hydrogen/LPG mixture. As the temperature rises in the combustion zone, the fresh incoming mixture has enough time to burn completely. The highest stabilization effect is achieved at a vane angle of 60°, which also aligns with the results of [25] at the same angle. Overall, it can be concluded that, for Type 1, an increase in the swirl number enhances flame stabilization. Similar results were obtained for Type 2, where maximum flame stabilization is also achieved at a 60° vane angle. However, flame stabilization for Type 2 is slightly lower than for Type 1. For instance, at a 30° vane angle and 0% hydrogen, φ_{LBO} values are 0.75 for Type 1 and 0.81 for Type 2. An increase in the hydrogen fraction leads to further stabilization. For Type 2, a 10% increase in hydrogen fraction results in a 46% improvement in stabilization. A larger recirculation zone involves more air in the combustion process, resulting in more complete fuel burnout and the better ignition of the fresh fuel–air mixture, which in turn increases flame stabilization. Increasing the vane angle to 45° further enhances stabilization. This is because a higher degree of

swirl, and consequently a higher swirl number, enlarges the recirculation zone (RZ), which boosts flame stabilization. This occurs because greater resistance to flame stretching allows the flame to better maintain its size, due to hydrogen combustion. The experiments confirm that increasing the hydrogen fraction significantly improves flame stabilization.

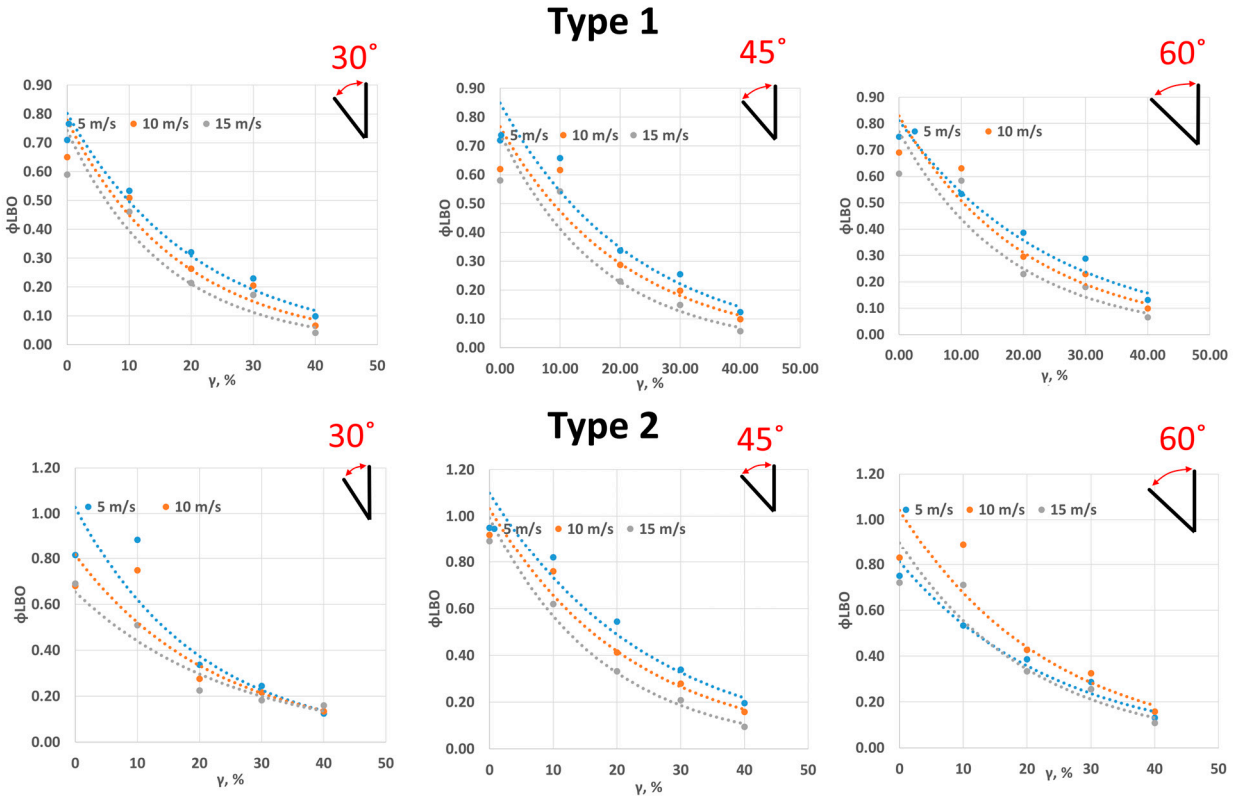

Figure 3. Dependence of flame stabilization on the vane angle and fraction of hydrogen.

Figure 4 shows the lean blow-off dependence at a constant hydrogen flow rate and its relation to the fuel feed type and the outlet vanes' swirl angle. As seen in the figure, the minimum stabilization is achieved at an angle of 30°. This occurs due to an insufficient mixing time for the LPG/H_2 mixture, as the fuel is fed directly to the base of the outlet vanes. This results in an increased mixing time, insufficient thermal stress in the zone, and reduced flame reactivity. In the case of Type 1, the LPG/H_2 mixture has a longer mixing time, considering that the fuel is fed in a narrow section, expanding later. These geometric features contribute to adequate fuel–air mixing, resulting in higher temperatures and a developed recirculation zone in the combustion area. This leads to increased stabilization. Similar results were found in [28], where an increase in the hydrogen fraction led to improved stabilization without flame swirl.

Lean blow-off occurs in two stages. In the first stage, heat release gradually decreases, leading to a drop in temperature in the combustion zone and a reduction in the ignition of the fresh mixture. This is followed by a second stage where the heat release decreases significantly. From this, we can conclude that as the swirl angle increases at a constant hydrogen concentration, the degree of swirl becomes crucial. An increase in the vane angle improves the mixture formation, causing the first stage of lean blow-off to occur at lower equivalence ratios.

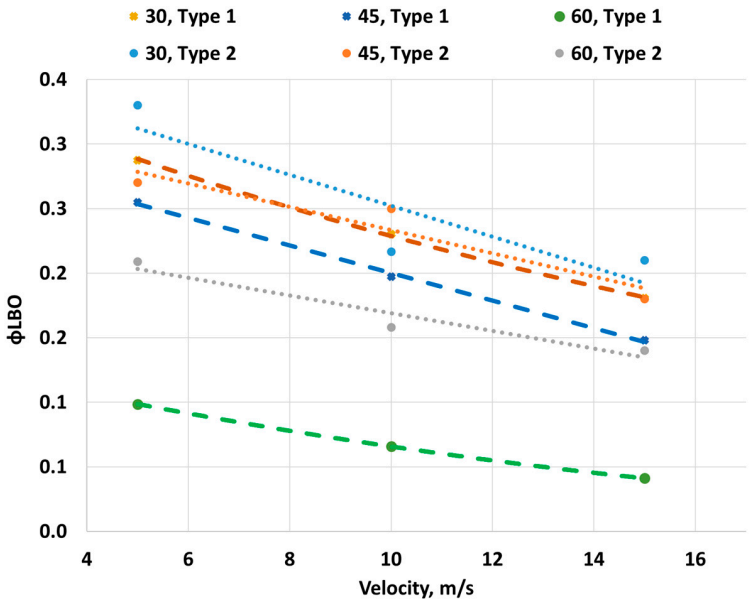

Figure 4. Lean blow-off dependence from vane angle at a constant hydrogen fraction value.

3.2. NOx, CO, and UHC Concentrations

Figure 5 shows the dependence of the NO_x concentration on the fuel feed type, hydrogen proportion, and outlet vane angle. For Type 1 at a 30° vane angle, the concentration ranges from 12 to 31 ppm. Additionally, an increase in the vane angle and equivalence ratio leads to a rise in NO_x concentration. A similar trend is observed for Type 1 at a 45° angle, where NO_x concentrations increase with a rising equivalence ratio. At a 45° vane angle, the concentration range for Type 1 falls between 13 and 33 ppm. A 10% increase in hydrogen proportion results in a 24% increase in NO_x concentration, which can be explained by the rise in combustion temperature and the more developed recirculation zone (RZ) [28,29].

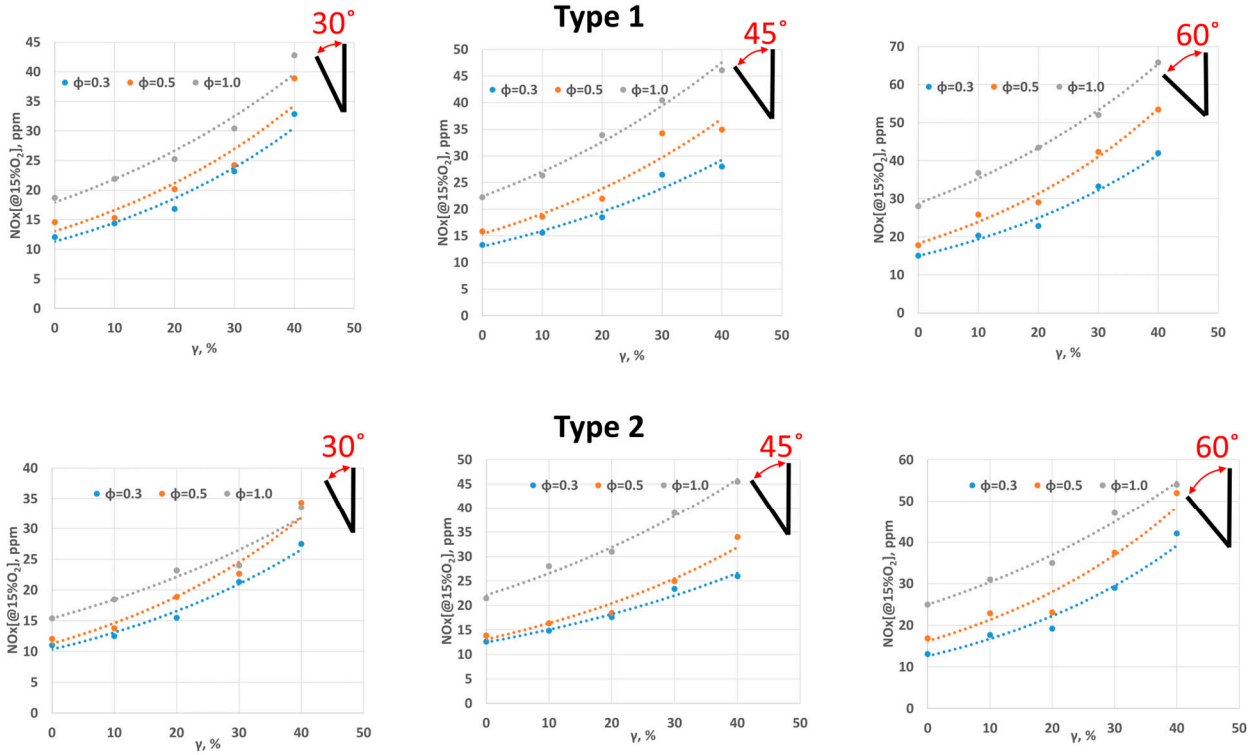

Figure 5. Dependence of NOx emissions on vane angle and fraction of hydrogen.

The maximum vane angle of 60° produces the highest NO_x concentrations. For Type 1 at a 60° angle, NO_x concentrations range from a minimum of 28 ppm to a maximum of 65 ppm. As the hydrogen proportion and vane angle increase, the flame temperature rises, and a well-developed RZ forms. These factors cause the gases to remain in the high-temperature zone for a longer period. As noted in [2], several factors contribute to the formation of nitrogen oxides, especially temperature, the degree of mixing, and the residence time of gases in the high-temperature zone. In this case, the two most influential factors are the high temperatures and prolonged residence time due to the developed RZ. Studies indicate that the maximum NO_x concentrations are achieved when approaching $\varphi = 1.0$. It is well known that under stoichiometric conditions, the mixture reaches its maximum temperature, which in turn increases NO_x formation. For Type 2 at a 30° vane angle, the NO_x concentration is lower, ranging from 11 to 27 ppm. Additionally, a 10% increase in hydrogen proportion results in an approximately 23% increase in NO_x concentration. The relatively lower NO_x concentrations in Type 2 are attributed to lower temperatures and the shorter residence times of the gases in the high-temperature zone. This is due to a shorter mixing time of the fuel with air, resulting in incomplete oxygen saturation, which leads to higher levels of incomplete combustion and consequently lower NO_x concentrations. A similar pattern is observed for the 45° vane angle, where a 10% increase in hydrogen proportion leads to a 22% rise in NO_x concentration. However, as the equivalence ratio increases, the rate of increase in NO_x concentration decreases. This is because a higher fuel proportion results in more unburned fuel, which does not fully participate in combustion. A similar conclusion can be drawn for the 60° vane angle. The increase in NO_x concentration is influenced by several factors. First, as the hydrogen proportion increases, the high-temperature zone shifts closer to the burner exit. Furthermore, an increase in hydrogen proportion raises the levels of free radicals such as O, OH, and H, which leads to a higher production of thermal NO, the main mechanism of NO_x formation.

Figure 6 shows the dependence of NO_x concentrations on the vane angle, equivalence ratio, and fuel introduction type. As observed, an increase in both the equivalence ratio and swirl angle leads to a rise in nitrogen oxide concentrations. The maximum NO_x concentrations for all configurations occur at a 60° vane angle. This can be explained by the fact that, at 60°, the most developed recirculation zone (RZ) is formed. Furthermore, the addition of hydrogen enhances the RZ's resistance to flame stretching, resulting in an increase in combustion temperature within the RZ [29]. A well-developed recirculation zone, combined with a high-combustion temperature, significantly contributes to the rise in nitrogen oxide concentrations. In this experiment, the maximum swirl angle of 60° corresponds to a swirl number (SW) of 1.0. Previous studies [27] on the effect of swirl number on NO_x concentrations indicate that the maximum NO_x concentrations are achieved at SW values between 0.75 and 1.4. This confirms that increasing SW to 1.3 (i.e., a 60° vane angle) leads to peak NO_x concentrations. Additionally, for Type 1, NO_x concentrations are 11% higher than for Type 2, likely due to the longer mixing time. With a strong RZ, meaning a strong swirl, increasing the proportion of hydrogen further elevates NO_x concentrations.

Figure 7 shows the dependence of CO concentrations on the vane angle, hydrogen concentration, and fuel feed type. For a 30° vane angle and Type 1, an increase in the proportion of hydrogen leads to a decrease in CO concentrations. The maximum CO concentration for the 30° angle and Type 1 is 330 ppm. An increase in the equivalence ratio results in higher CO concentrations in the exhaust gases. Increasing the vane angle to 45° leads to a slight decrease in CO concentrations, with the maximum CO concentration at a 45° angle being 294 ppm at $\varphi = 1.0$. Lower CO concentrations were observed at a 60° angle. The primary mechanism for CO formation is insufficient temperature and inefficient mixing of the fuel with the oxidizer [2]. An increase in the degree of swirl, due to the vane angle, creates a high-temperature zone where air mixes with the fuel, enhancing the oxidation of carbon and raising the temperature. On the other hand, another factor

influencing CO formation is the cooling of gases in the near-wall region. Due to hydrogen's high reactivity and wide combustion zone, these "parasitic" zones become smaller at higher swirl levels, which positively impacts the reduction in CO concentrations. For Type 2 at a 30° angle, there is a more linear decrease in CO concentrations, with the maximum values achieved at γ = 0%. This is attributed to lower temperatures compared to scenarios where hydrogen is added, leading to less complete combustion reactions. Increasing the swirl degree further reduces CO concentrations. Compared to a 30° angle, the maximum CO concentration decreases by 5%. In all configurations, an increase in the equivalence ratio leads to higher CO concentrations in the exhaust gases. The lowest CO concentrations are observed at a 60° swirl, which can be explained by the developed recirculation zone, where combustion reactions are more complete due to the high proportion of air entering from the surroundings of the recirculation zone.

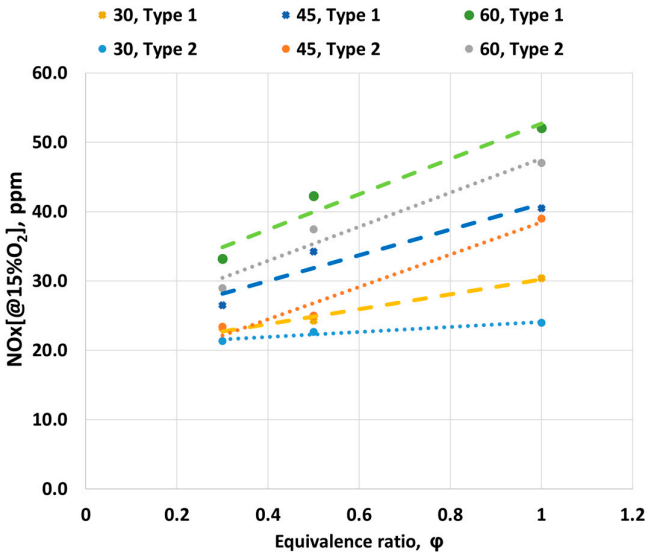

Figure 6. Dependence of NOx emissions on the vane angle.

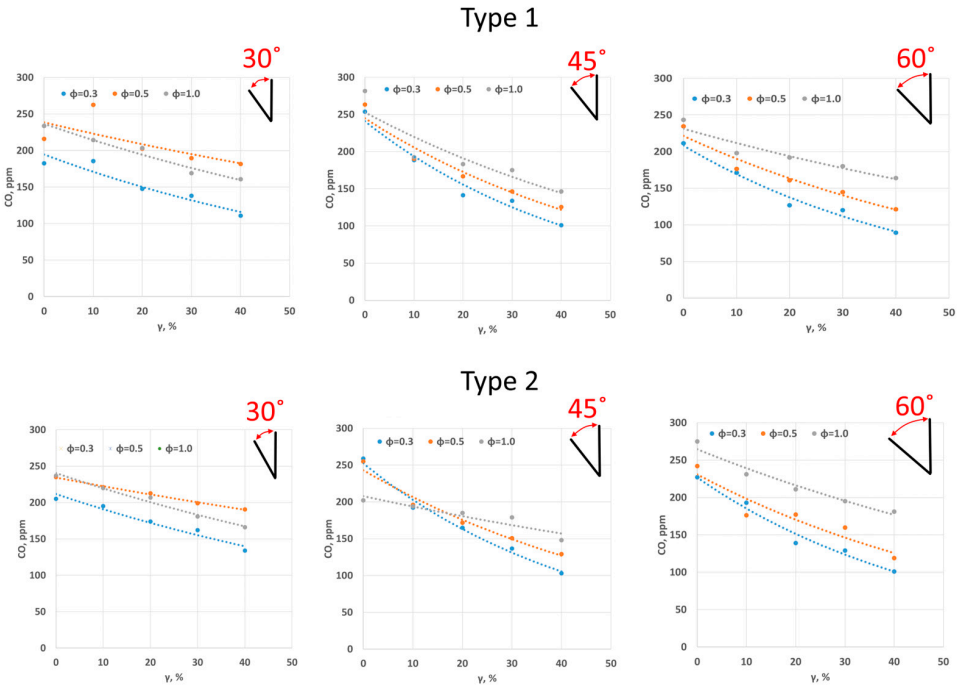

Figure 7. Dependence of CO emissions on the vane angle and fraction of hydrogen.

Figure 8 shows the dependence of the CO concentration on the equivalence ratio and vane angles. As seen in the figure, increasing the equivalence ratio in all variants leads to a rise in CO concentration. In general, increasing the vane angle reduces CO concentrations. At γ = 30%, Type 1 exhibits 3–5% lower CO concentrations. The studies demonstrate that flow swirl has a greater effect on NO_x concentrations than on CO concentrations. The lowest CO concentrations are observed at a 60° vane angle for Type 1, which can be attributed to the longer mixing period resulting from the fuel being supplied through a tube. Additionally, the fuel supply method may influence this, as the fuel is sprayed radially through four holes, promoting the deeper penetration of the fuel into the air stream.

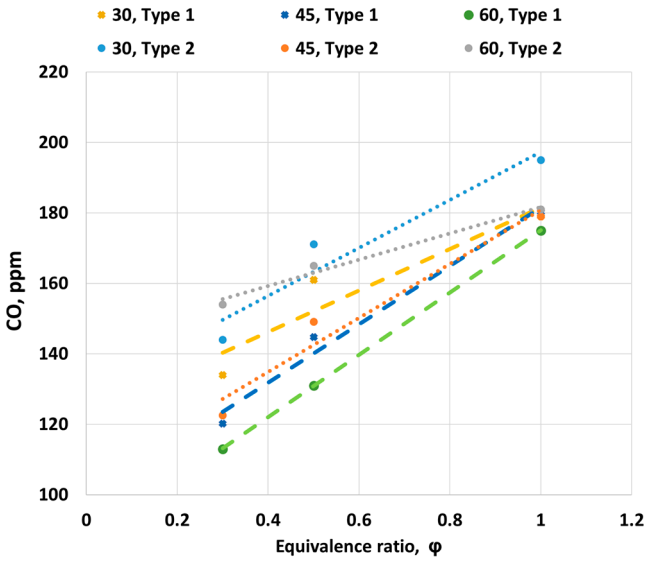

Figure 8. Dependence of CO emissions on the vane angle.

3.3. Flame Shape

Figure 9 shows flame photographs at γ = 30%. As seen in the figure, the flame is more transparent compared to the previous photographs. For Type 1, a more uniform temperature distribution is observed, although the significant heating of the blade surface is also noticeable, especially on the lower left side. The authors did not measure the blade temperature profile. When Type 2 fuel is supplied, a blue rim is observed around the base of the blade assemblies. It should be noted that high temperatures were observed in this LPG/H_2 supply area.

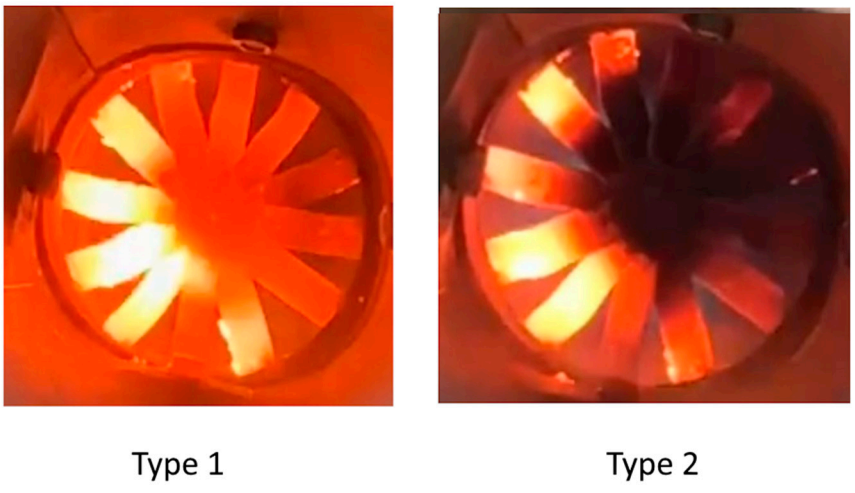

Figure 9. Flame shape dependence on the vane angle.

4. Conclusions

This study examined the concentrations of NO_x and CO along with flame stabilization indices under the influence of hydrogen (H_2) enrichment in LPG. It also evaluated the impact of fuel supply methods on combustion parameters. The findings revealed that flame stabilization indices are significantly affected by both the degree of swirl and the proportion of hydrogen in the fuel. The swirl promotes the formation of a recirculation zone (RZ) in the combustion area, and higher swirl intensity enhances fuel combustion efficiency, leading to improved flame stability. Additionally, the stabilization of the flame improves as the hydrogen proportion increases.

The analysis of NO_x concentrations shows that NO_x emissions increase with a higher hydrogen content and swirl intensity. This trend is attributed to the high reactivity of hydrogen and elevated temperatures in the recirculation zone. The choice of fuel supply method also plays a critical role: Type 1 results in higher NO_x levels due to longer mixing times between fuel and air, while Type 2, with a 30° vane angle, yields lower NO_x concentrations (11–27 ppm). A 10% increase in hydrogen proportion raises NO_x emissions by approximately 23%. Lower NO_x concentrations for Type 2 are associated with reduced temperatures and shorter gas residence times in the high-temperature zone.

In terms of CO emissions, the results indicate a reduction in CO levels with increased hydrogen content and swirl intensity, driven by higher combustion temperatures that enhance carbon oxidation. The fuel supply method also influences CO emissions: larger vane angles decrease CO concentrations. At a swirl ratio of γ = 30%, Type 1 shows 3–5% lower CO levels compared to Type 2. The lowest CO concentrations are observed at a 60° vane angle with Type 1. However, using Type 2 results in higher CO emissions due to lower combustion temperatures and the insufficient mixing of fuel and air, leading to localized oxidizer shortages.

This study demonstrates that increasing the proportion of hydrogen in LPG significantly enhances flame stabilization. This improvement is attributed to the elevated temperatures in the combustion zone, which promote the more efficient ignition of the fresh fuel–air mixture. In the case of Type 1 configuration, a vane angle of 30° achieves high flame stabilization at lower velocities. However, increasing the velocity reduces flame stabilization by approximately 8%. Furthermore, for every 10% increase in the hydrogen fraction, flame stabilization improves by an average of 32%.

These findings highlight the importance of optimizing the hydrogen proportion, swirl intensity, and operating conditions to achieve stable combustion. While a higher hydrogen content enhances stabilization, care must be taken to balance the fuel supply parameters and flow velocities to avoid adverse effects, such as increased NO_x emissions. In conclusion, while both NO_x and CO emissions are influenced by hydrogen enrichment and swirl intensity, swirl has a more pronounced effect on NO_x concentrations. Achieving optimal combustion performance requires balancing fuel composition, swirl intensity, and the appropriate fuel supply method to minimize emissions while maintaining flame stability.

Author Contributions: Conceptualization, A.M.D.; methodology, D.R.U. and A.K.Y.; software, D.R.U. and A.K.Y.; validation, A.M.D. and Z.A.A.; formal analysis, A.K.Y.; investigation, M.B.K. and Z.S.D.; resources, A.M.D.; data curation, M.B.K.; writing—original draft preparation, D.R.U.; writing—review and editing, D.R.U. and A.K.Y.; visualization, D.R.U. and N.R.K.; supervision, A.M.D.; project administration, A.M.D.; funding acquisition, A.M.D. and A.S.B. All authors have read and agreed to the published version of the manuscript.

Funding: This research was funded by the Science Committee of the Ministry of Science and Higher Education of the Republic of Kazakhstan (Grant No. AP14872041).

Data Availability Statement: Raw data can be provided by the corresponding and first author (D.N.) upon reasonable request.

Conflicts of Interest: The authors declare no conflicts of interest.

References

1. On Approval of the Strategy for Achieving Carbon Neutrality of the Republic of Kazakhstan Until 2060. Decree of the President of the President of the Republic of Kazakhstan dated February 2, 2023 No. 121. Available online: https://climateactiontracker.org/countries/kazakhstan/net-zero-targets/ (accessed on 25 September 2024).
2. Lefebvre, A. *Gas Turbine Combustion*; Hemisphere Publishing: London, UK, 1983; p. 550.
3. Xu, Z.; Yang, G.; Sheng, Z.; Sun, H.; Yang, X.; Ji, S. Large eddy simulation of premixed hydrogen-air combustion characteristics in closed space with different shrinkage rate. *Int. J. Hydrogen Energy* **2024**, *81*, 280–291.
4. Emre, B.; Dilay, G.; Mehmet, K.; Christophe, A.; İskender, G. Numerical and experimental investigations of swirl-stabilized partially premixed flames using natural gas-hydrogen-air mixtures. *Appl. Therm. Eng.* **2024**, *254*, 123830.
5. Cui, Y.; Liu, F.; Cao, S.; Ma, Y.; Niu, Y.; Zhao, D. Experimental study of emission characteristics for fully premixed combustion of dimethyl ether and hydrogen based on flame ions. *J. Energy Inst.* **2024**, *114*, 101654. [CrossRef]
6. Concetti, R.; Hasslberger, J.; Chakraborty, N.; Klein, M. Effects of liquid water addition on turbulent premixed hydrogen/air combustion. *Fuel* **2024**, *373*, 132–314. [CrossRef]
7. Bertsch, J.; Poinsot, T.; Bertier, N.; Ruan, J.L. Stabilization regimes and flame structure at the flame base of a swirled lean premixed hydrogen–air injector with a pure hydrogen pilot injection. *Proc. Combust. Inst.* **2024**, *40*, 105660. [CrossRef]
8. Li, H.; Li, M.; Chu, G.; Xiao, H. Experimental investigation and model analysis of non-premixed hydrogen jet flames. *Int. J. Hydrogen Energy* **2024**, *in press*. [CrossRef]
9. Nemitallah, M.A.; Abdelhalim, A.; Abdelhafez, A.; Mohamed, A.H. Experimental and numerical study on flow/flame interactions and pollutant emissions of premixed methane-air flames with enhanced lean blowout hydrogen injection. *Int. J. Hydrogen Energy* **2024**, *65*, 14–32. [CrossRef]
10. Ji, L.; Zhang, W.; Wang, J.; Huang, Z.; Bai, X.S. Effects of secondary hydrogen injection on thermoacoustic instability of swirling premixed flames in a model combustor. *Fuel* **2024**, *377*, 132722. [CrossRef]
11. Howarth, T.L.; Day, M.S.; Pitsch, H.; Aspden, A.J. Thermal diffusion, exhaust gas recirculation and blending effects on lean premixed hydrogen flames. *Proc. Combust. Inst.* **2024**, *40*, 105429. [CrossRef]
12. Gaucherand, J.; Laera, D.; Schulze-Netzer, C.; Poinsot, T. Intrinsic instabilities of hydrogen and hydrogen/ammonia premixed flames: Influence of equivalence ratio, fuel composition and pressure. *Combust. Flame* **2023**, *256*, 112986. [CrossRef]
13. Porcarelli, A.; Kruljević, B.; Langella, I. Suppression of NO_x emissions by intensive strain in lean premixed hydrogen flamelets. *Int. J. Hydrogen Energy* **2024**, *49*, 413–431. [CrossRef]
14. Tamadonfar, P.; Karimkashi, S.; Zirwes, T.; Vuorinen, V.; Kaario, O. A numerical study on premixed laminar ammonia/air flames enriched with hydrogen: An analysis on flame–wall interaction. *Combust. Flame* **2024**, *265*, 113444. [CrossRef]
15. Francolini, B.; Fan, L.; Abbasi-Atibeh, E.; Bourque, G.; Vena, P.; Bergthorson, J. Investigation of differential diffusion in lean, premixed, hydrogen-enriched swirl flames. *Appl. Energy Combust. Sci.* **2024**, *18*, 100272. [CrossRef]
16. Merotto, L.; Balmelli, M.; Soltic, P. Hydrogen direct injection: Optical investigation of premixed and jet-guided combustion modes. *Int. J. Hydrogen Energy* **2024**, *61*, 284–295. [CrossRef]
17. Sathish, T.; Karthikeyan, S.; Sathyamurthy, R.; Rajaram, K.; Kumar, S.; Kumar, P.; Giri, J.; Kassian, T.J.; Amesho, T. Synergistic effects of nano-enhanced waste transformer oil and hydrogen premixing on CI engine performance and emissions. *Int. J. Hydrogen Energy* **2024**, *56*, 484–497. [CrossRef]
18. Chen, W.; He, W.; Ma, Y.; Yu, S.; Zuo, Q.; Kou, C.; Ning, D.; Gong, S.; Wang, H.; Zhu, G. Numerical Investigation of flow and combustion process in a hydrogen direction injection rotary engine. *Fuel* **2024**, *379*, 133100. [CrossRef]
19. Aravindan, M.; Kumar, G.P.; Arulanandam, M.K.; Murali, S.; Sheoran, N.; Waykole, N.; Muthaiah, R.; Sharma, P. Multi-objective optimization and analysis of chemical kinetics properties: Exploring the impact of different hydrogen blending ratios on LPG and methane-air mixtures. *Energy Convers. Manag. X* **2024**, *22*, 100532.
20. Kacem, S.H.; Jemni, M.A.; Driss, Z.; Abid, M.S. The effect of H_2 enrichment on in-cylinder flow behavior, engine performances and exhaust emissions: Case of LPG-hydrogen engine. *Appl. Energy* **2016**, *179*, 961–971. [CrossRef]
21. Lu, C.; Chen, W.; Zuo, Q.; Kou, C.; Wang, H.; Xiao, G.; Zhu, G.; Ma, Y. Numerical investigation on gaseous fuel injection strategies on combustion characteristics and NO emission performance in a pure hydrogen engine. *Fuel* **2024**, *363*, 130911. [CrossRef]
22. Chen, W.; Lu, C.; Zuo, Q.; Kou, C.; Shi, R.; Wang, H.; Ning, D.; Shen, Z.; Zhu, G. Combustion characteristics analysis and performance evaluation of a hydrogen engine under direct injection plus lean burn mode. *J. Clean. Prod.* **2024**, *470*, 143323. [CrossRef]
23. Guo, H.; Smallwood, G.J.; Liu, F.; Ju, Y.; Gülder, Ö.L. The effect of hydrogen addition on flammability limit and NO_x emission in ultra-lean counterflow CH4/air premixed flames. *Proc. Combust. Inst.* **2005**, *30*, 303–311. [CrossRef]
24. Abdelhalim, A.; Abdelhafez, A.; Nemitallah, M.A. Effects of non-premixed H_2 injection on the stability, shape, and combustion/emissions characteristics of premixed CH4/air flames: An experimental study. *Fuel* **2024**, *365*, 131213. [CrossRef]
25. Dostiyarov, A.M.; Umyshev, D.R.; Kibarin, A.A.; Yamanbekova, A.K.; Tumanov, M.E.; Koldassova, G.A.; Anuarbekov, M.A. Experimental Investigation of Non-Premixed Combustion Process in a Swirl Burner with LPG and Hydrogen Mixture. *Energies* **2024**, *17*, 1012. [CrossRef]
26. Duissenbek, Z.; Ozhikenova, Z.; Umyshev, D.; Dostiyarov, A. Torch Burner. KZ Patent 34972, filed 13 December 2019, 18 April 2021.

27. Dostiyarov, A.; Umyshev, D.; Kumargazina, M.; Kibarin, A.; Yamanbekova, A. Burner Device for Combustion of Natural Gas with Hydrogen Additive. KZ Patent 36843, Filed 3 March 2023, 12 July 2024.
28. Wang, B.; Qiu, R.; Jiang, Y. Effects of Hydrogen Enhancement in LPG/Air Premixed Flame. *Acta Phys.-Chim. Sin.* **2008**, *24*, 1137–1142. [CrossRef]
29. Sungwoo, P. Hydrogen addition effect on NO formation in methane/air lean-premixed flames at elevated pressure. *Int. J. Hydrogen Energy* **2021**, *46*, 25712–25725.